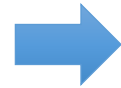
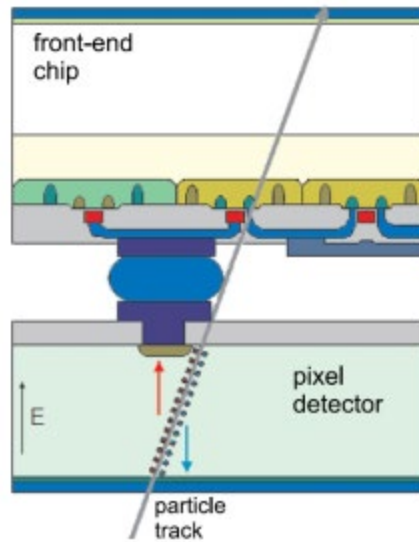




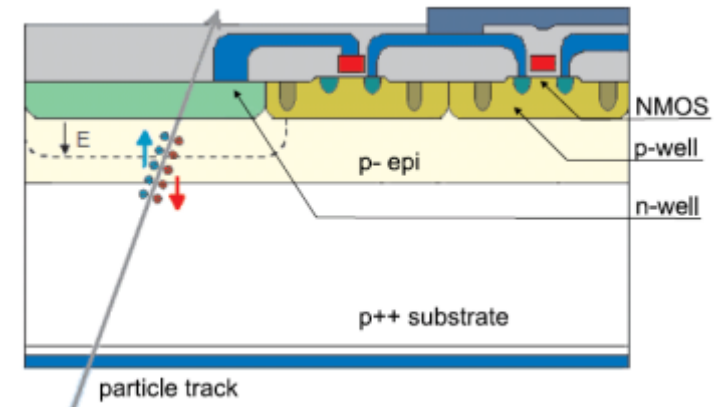
Rivelatori e Apparati

Slides_8 – MAPS, LGAD, SiPM, Calorimetri

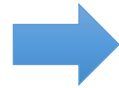
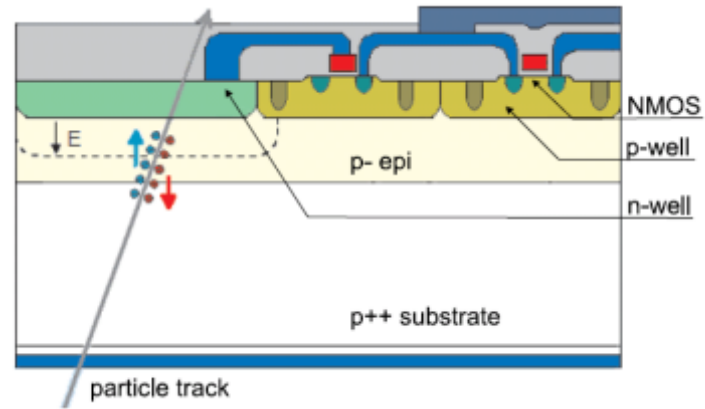
Hybrid Pixel Detectors



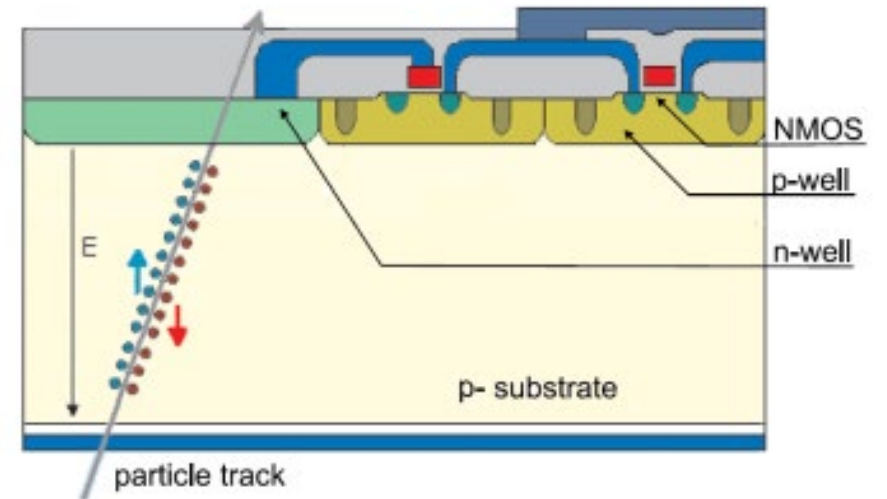
Monolithic Pixels



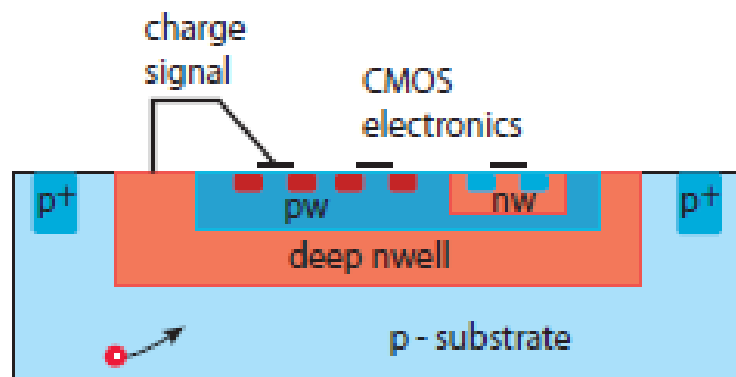
Monolithic Pixels



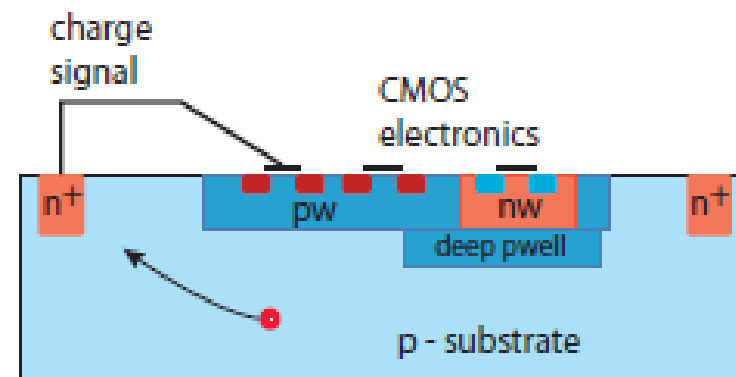
Depleted Monolithic Pixels



Fill factor

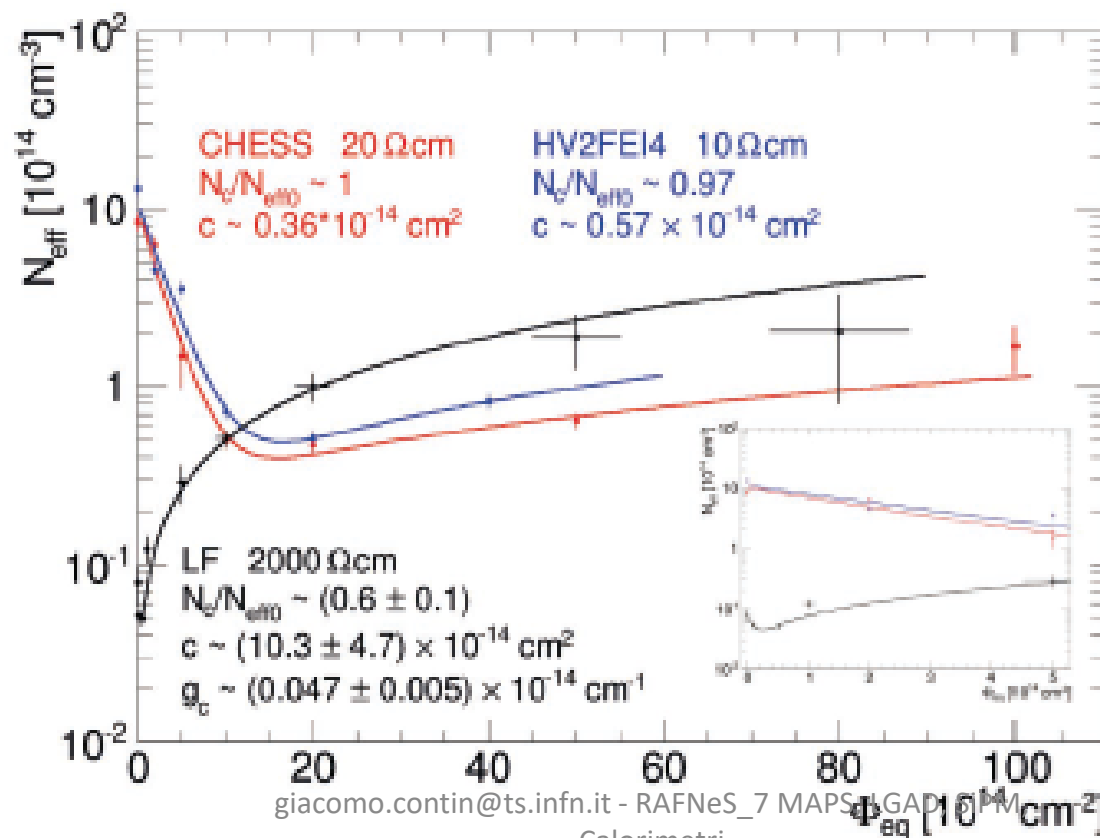


(a) Large fill-factor



(b) Small fill-factor

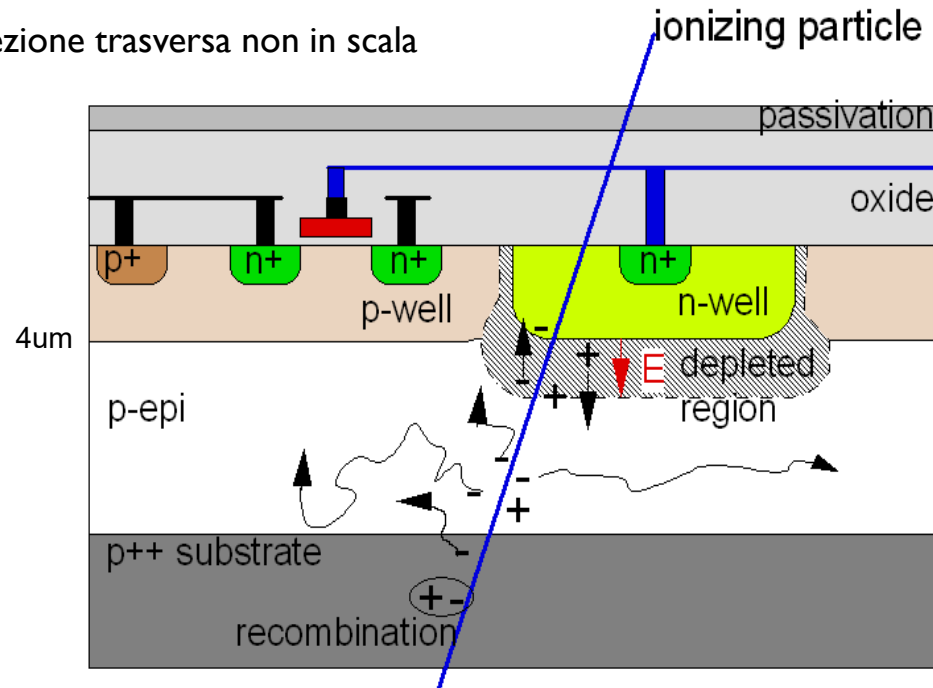
Resistività' substrato



La tecnologia MAPS

Volume sensibile e logica CMOS di prima elaborazione del segnale nello stesso cristallo di silicio

Sezione trasversa non in scala



- ▶ Monolithic Active Pixel Sensor
- ▶ Tecnologia industriale standard CMOS
- ▶ **Room temperature** operation
- ▶ Sensore e processazione del segnale integrati nello stesso silicio
- ▶ Il segnale e' creato nell'epitassiale (tipicamente $\sim 10-15 \mu\text{m}$) a basso drogaggio \rightarrow segnale di un MIP limitato a < 1000 elettroni
- ▶ La raccolta di carica avviene soprattutto per diffusione termica (lenta, $\sim 100 \text{ ns}$), anche grazie ai confini "riflettenti" reflective boundaries at p-well and substrate.
- ▶ Epitassiali ad alta resistivita' per ottenere zone svuotate piu' spesse \rightarrow raccolta della carica piu' efficiente, piu' tollerante alle radiazioni
- ▶ 100% fill-factor

STAR HFT PXL sensor: Ultimate-2

- ▶ *Ultimate-2*: third generation sensor developed for PXL by the PICSEL group of IPHC, Strasbourg
- ▶ *Monolithic Active Pixel Sensor* technology, MIMOSA series

• High resistivity p-epi layer

- Reduced charge collection time
- Improved radiation hardness

• S/N ~ 30

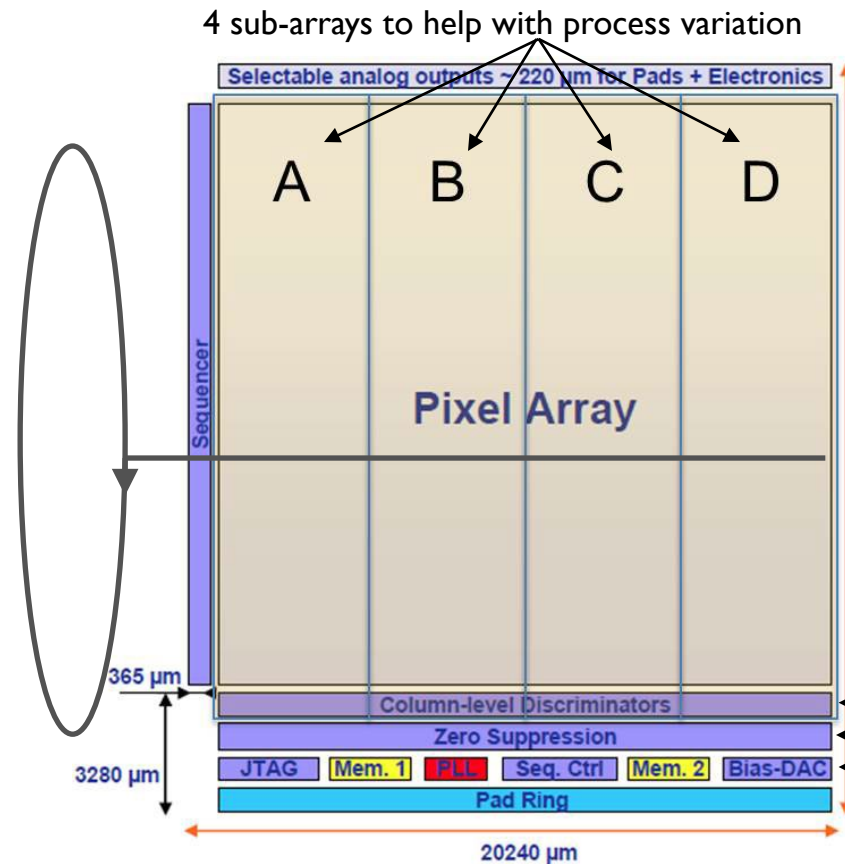
• MIP Signal ~ 1000 e-

• Rolling-shutter readout

- A row is selected
- For each column, a pixel is connected to discriminator
- Discriminator detects possible hit
- Move to next row

• 185.6 μ s integration time

• ~170 mW/cm² power dissipation



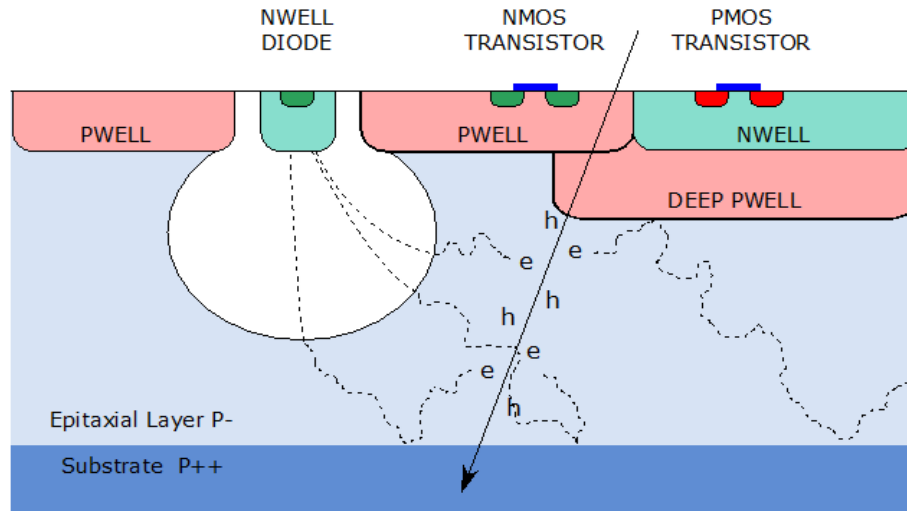
▶ Pixel matrix

- ▶ 928 rows * 960 columns = ~1M pixel
- ▶ In-pixel amplifier
- ▶ In-pixel Correlated Double Sampling (CDS)

▶ Digital section

- ▶ End-of-column discriminators
- ▶ Integrated zero suppression (up to 9 hits/row)
- ▶ Ping-pong memory for frame readout (~1500 w)
- ▶ 2 LVDS data outputs @ 160 MHz

CMOS Pixel Sensor using TowerJazz 0.18 μm CMOS Imaging Process

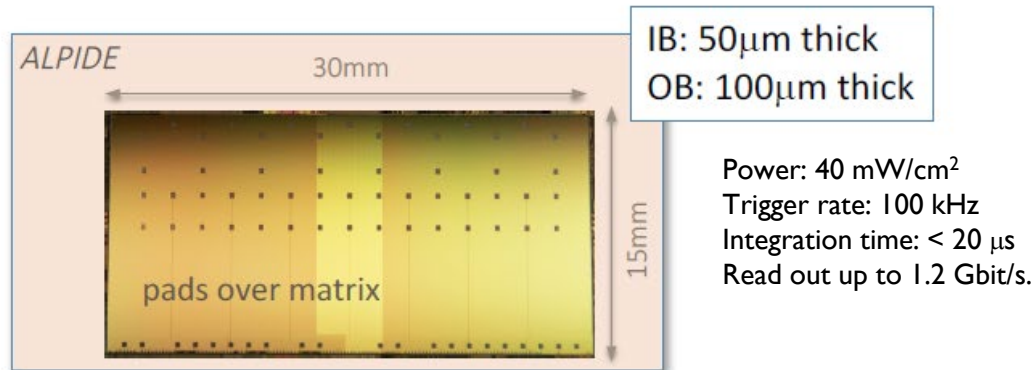
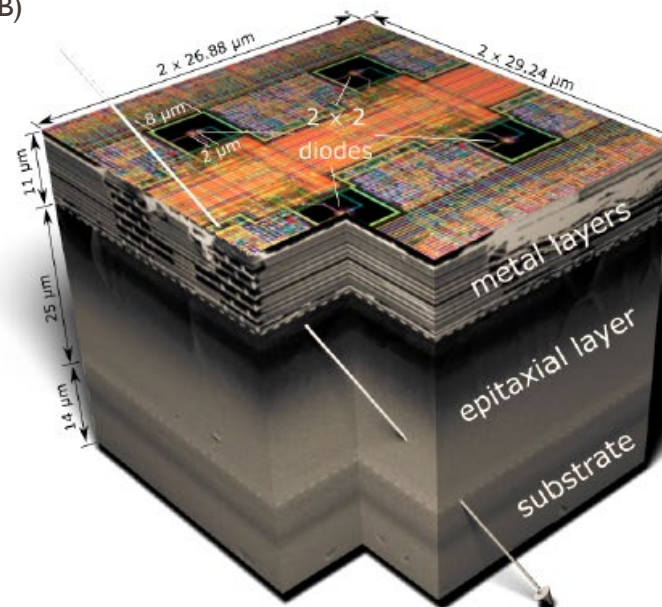
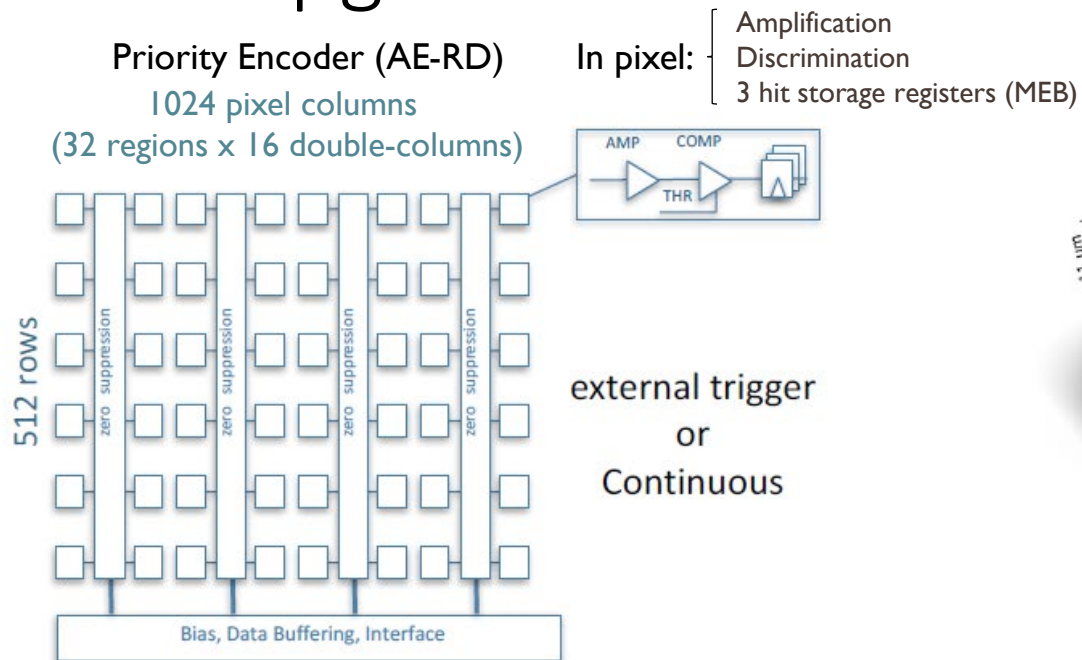


ALPIDE sensor (developed within ALICE)

- $\sim 28 \mu\text{m}$ pitch
- Integration time: $< 20 \mu\text{s}$
- Trigger rate: 100 kHz
- Read out up to 1.2 Gbit/s
- Power: 40 mW/cm²
- Priority encoder - sparsified readout
- Rad.Tolerant: 700krad - 10^{14} IMeV $n_{\text{eq}}/\text{cm}^2$

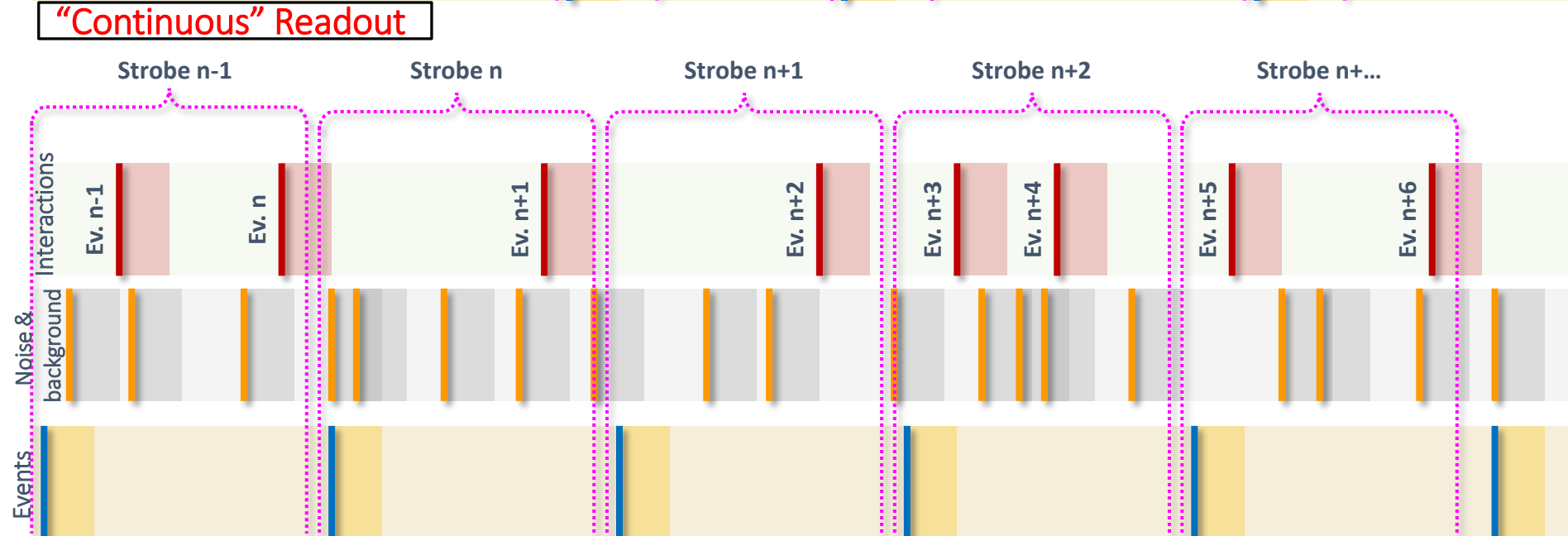
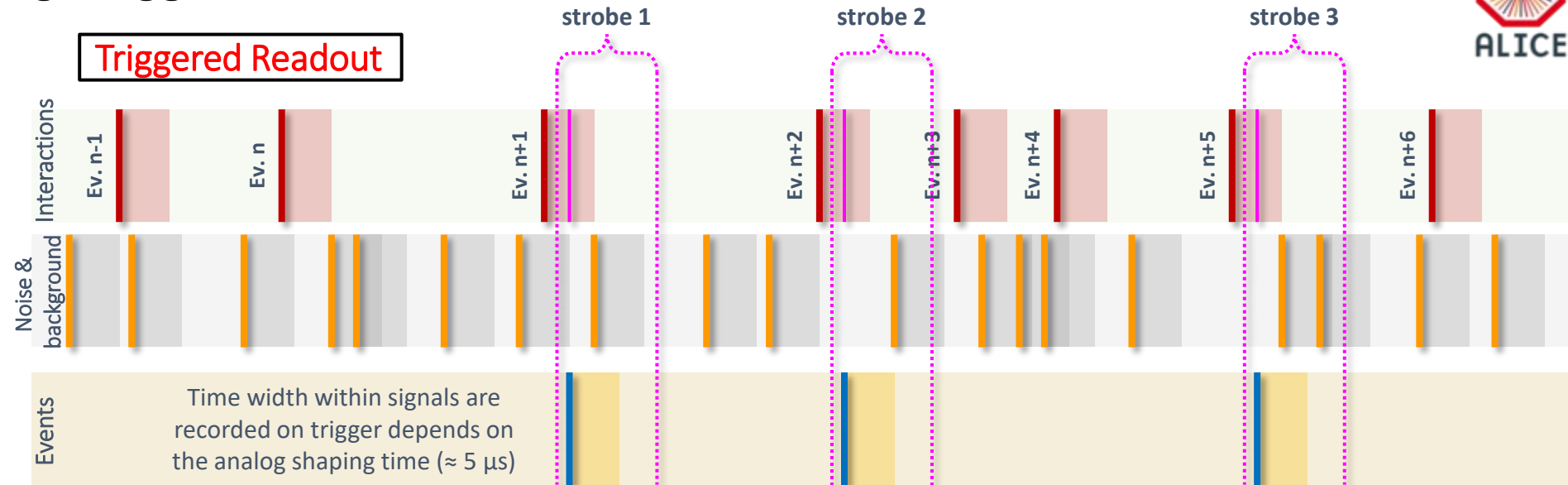
- ▶ High-resistivity ($> 1\text{k}\Omega \text{ cm}$) p-type epitaxial layer ($20\mu\text{m} - 40\mu\text{m}$ thick) on p-type substrate
- ▶ Small n-well diode ($2-3 \mu\text{m}$ diameter), ~ 100 times smaller than pixel \Rightarrow low capacitance
- ▶ Application of (moderate) reverse bias voltage to substrate can be used to increase depletion zone around NWELL collection diode
- ▶ Quadruple well process: deep PWELL shields NWELL of PMOS transistors, allowing for full CMOS circuitry within active area

ALICE ITS Upgrade sensor: ALPIDE



130,000 pixels / cm² 27x29x25 μm³
 spatial resolution: ~ 5 μm (3-D)
 Max particle rate: 100 MHz / cm²
 fake-hit rate: ~ 10⁻¹⁰ pixel / event
 power : ~ 300 nW / pixel

ALPIDE Timing: Triggered & "Continuous" Readout



Rivelatori al silicio per misure di tempo

Si basano sulla moltiplicazione a valanga delle cariche in movimento nel semiconduttore

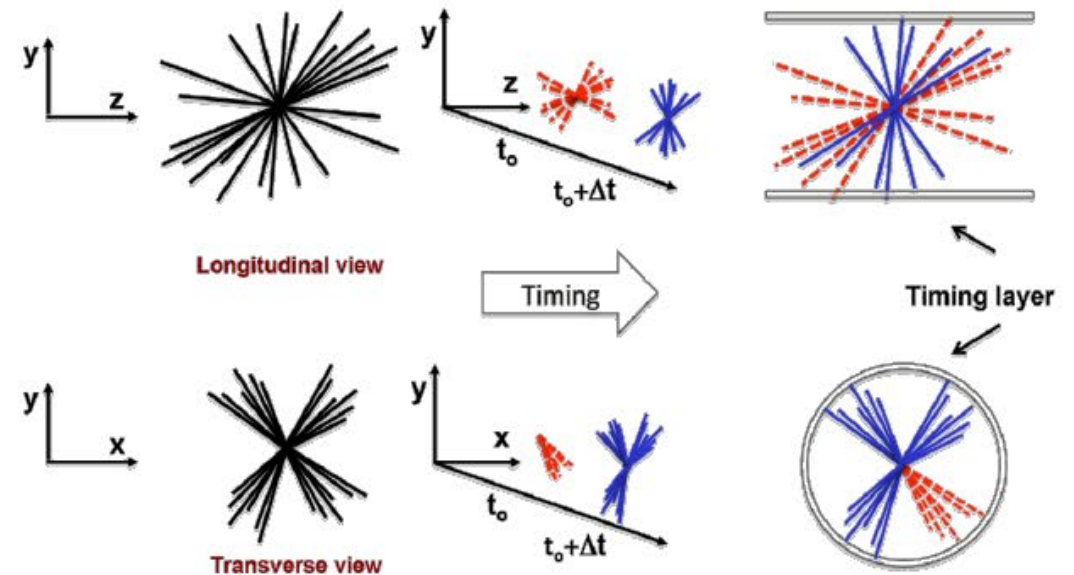
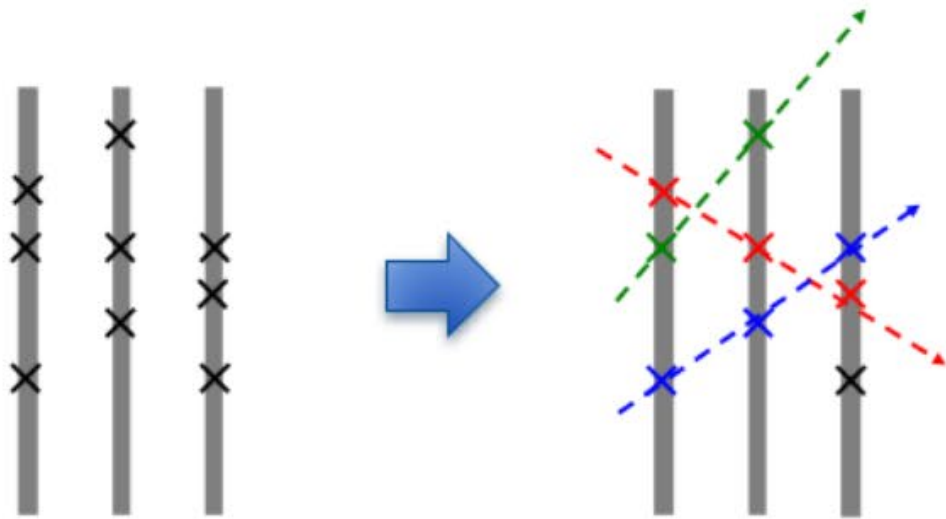
- Low Gain Avalanche Detectors (LGAD):
 - Rivelatori a valanga a basso guadagno tramite un sottile strato p+ ad alta concentrazione vicino all'anodo di raccolta
 - Gain: ~ 10
- Avalanche Photon Detectors (APD) & Single photon avalanche photodiode (SPAD)
 - Fotodiode usato in regime valanga, come un interruttore seguito da una resistenza di quenching che spegne la valanga
 - Gain: ~ 1000
- Silicon Photo-Multiplier (SiPM)
 - Matrici di SPAD in parallelo, non usato per immagine perché somma i segnali dalle diverse celle
 - Gain: ~ 10000

Caratteristiche degli LGAD

- Guadagno basso:
 - Permette un rumore piu' basso, crea campi meno intensi e quindi la possibilita' di segmentare di piu' la superficie, limita la dissipazione di potenza anche dopo irraggiamento
 - Se usato per particelle cariche, il segnale abbastanza alto permette di avere un buon S/N anche con un guadagno $\sim 10-20$
- Spessore sottile:
 - La durata del segnale generato dipende unicamente dal tempo massimo di deriva di un elettrone da una parte all'altra del silicio. L'ampiezza dipende dal fattore di guadagno. Quindi con guadagno fisso, la pendenza del fronte di salita aumenta per spessori piu' sottili.
 - D'altro canto spessori sottili introducono capacita' di carico maggiore, che poi necessitano di alti gain per misurare con precisione il segnale nell'elettronica. Entrambi i fattori creano un rumore piu' alto
- Ottimali: Gain: ~ 20 – Spessore: ~ 50 μm

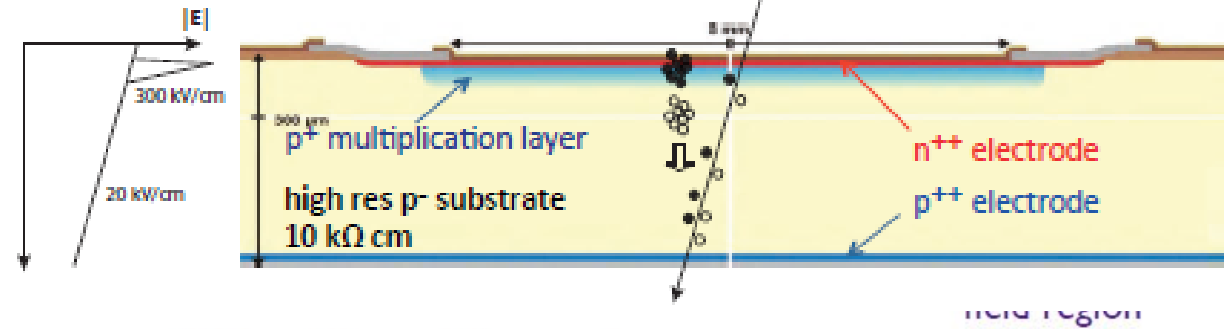
Acquisition of timing information

- Time tagging at each point
 - LHCb Upgrade II (Run 5 ~2030)
- Timing in the event reconstruction
 - HL-LHC: ATLAS and CMS



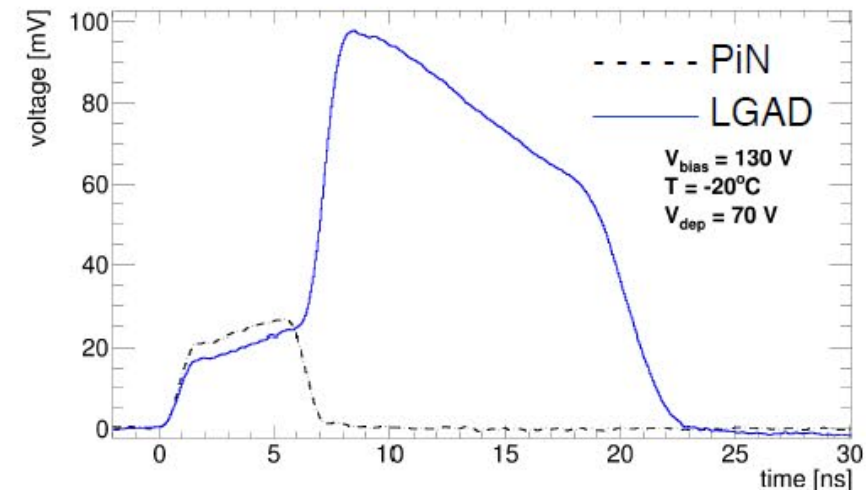
Gain mechanism in LGADs

- Planar silicon sensors (n+/p/p-)
 - n+ implant, p substrate
 - p-type multiplication layer



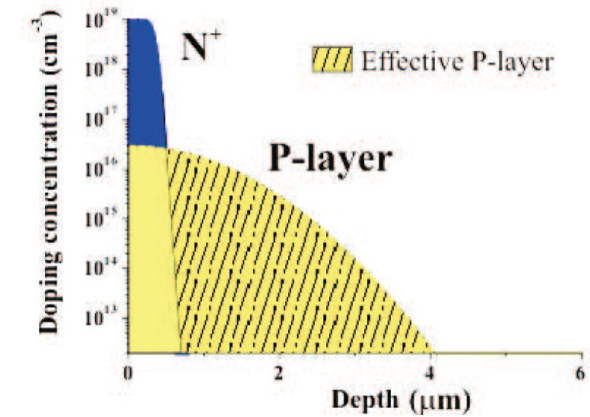
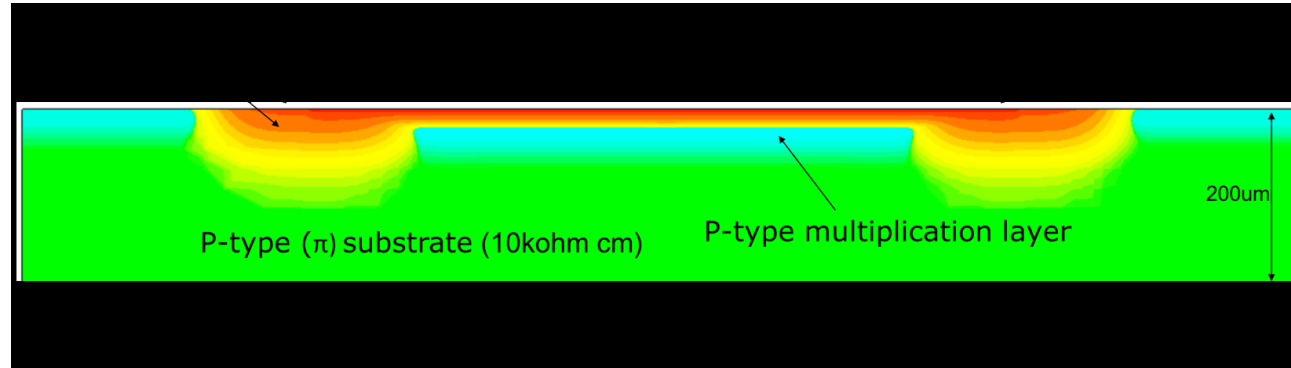
- **High electric field region in the multiplication layer**

- Charges undergo impact ionisation
- Gain depends on:
 - multiplication layer doping
 - bias voltage
 - temperature

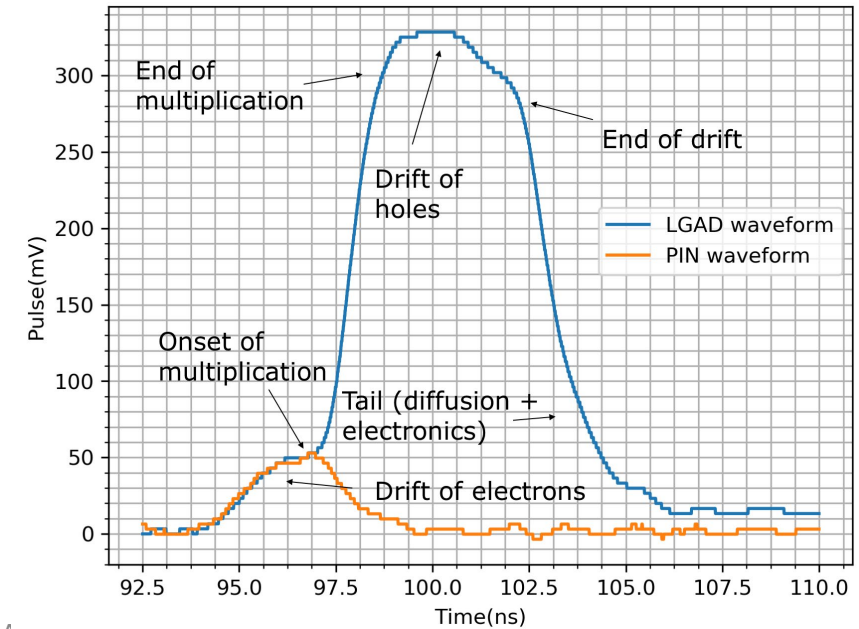
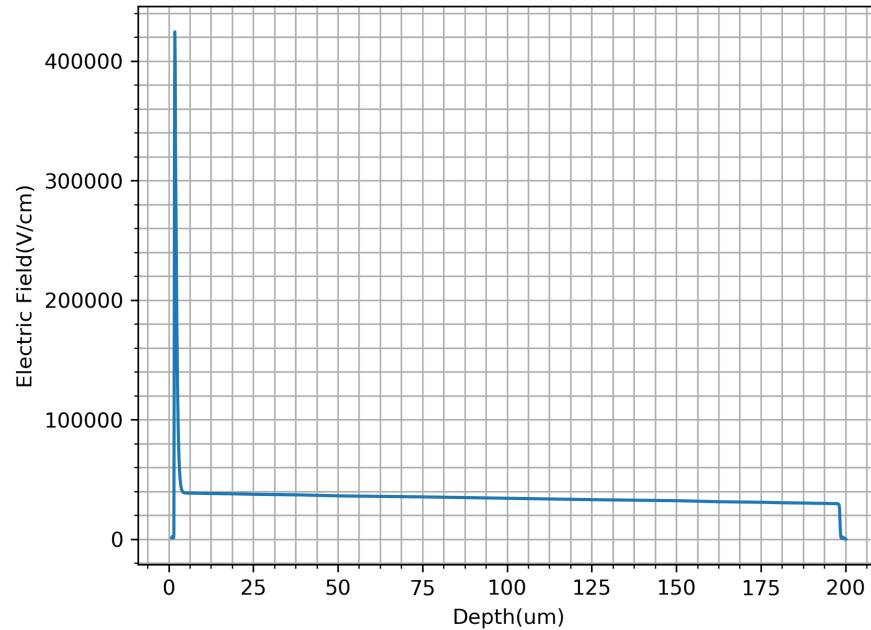


S. Otero Ugobono et al., IEEE TNS (2018) vol. 6, no. 8, pp. 1667-1675

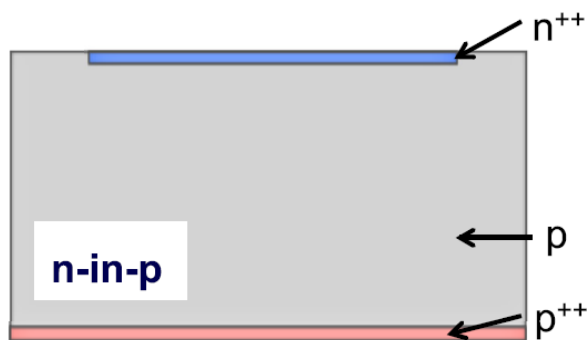
LGAD: simulazioni



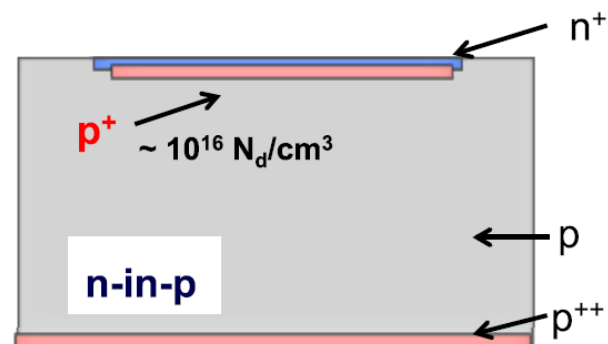
Electric Field Profile across junction



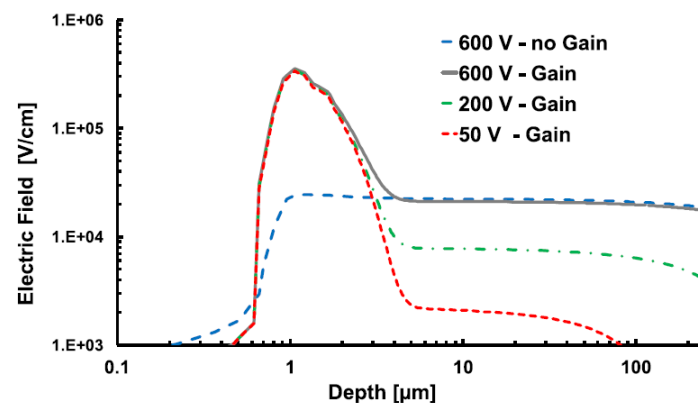
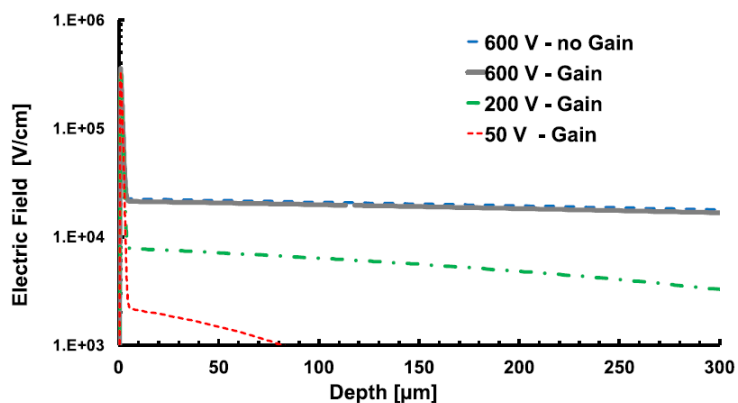
Campo elettrico in confronto a giunzione standard



Traditional silicon detector

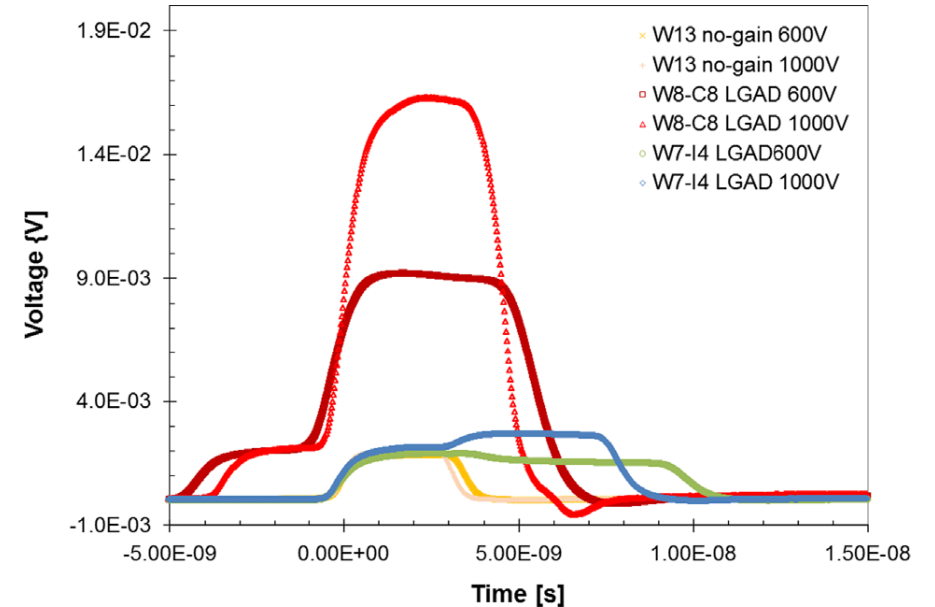
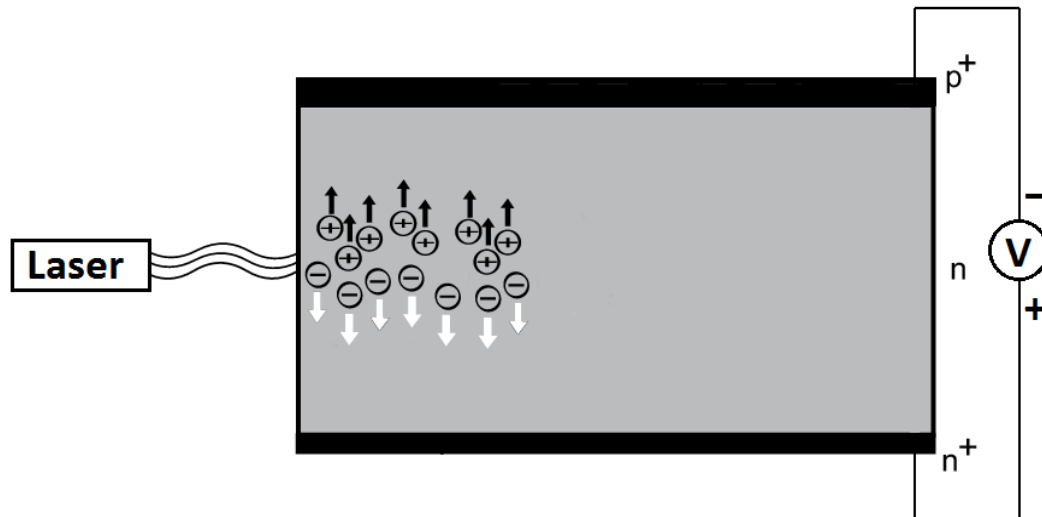


Low gain avalanche detectors



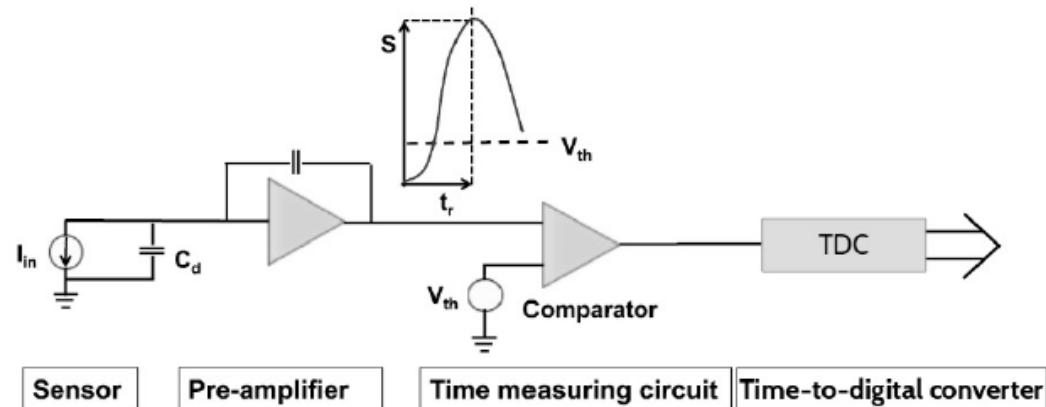
Caratterizzazione LGAD: misure TCT

- Principio di funzionamento (Edge-)Transient Current Technique
- Misura TCT su LGAD con diversi Guadagni e a diverse Vbias



Localizzazione della generazione di carica per descrivere il profilo di drogaggio e gli effetti sulla valanga

Time resolution



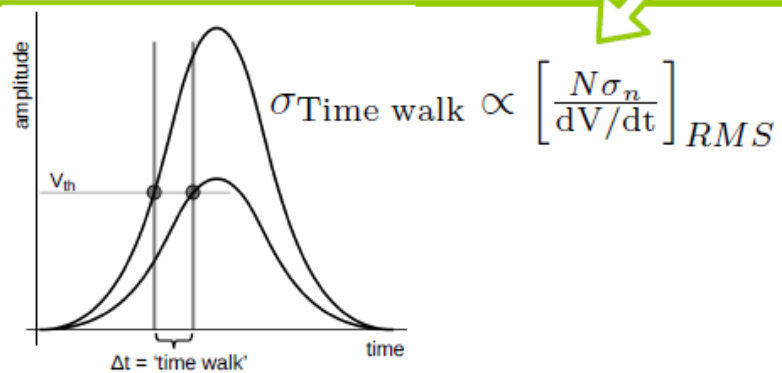
$$\sigma_t^2 = \sigma_{\text{Time walk}}^2 + \sigma_{\text{Landau noise}}^2 + \sigma_{\text{Jitter}}^2 + \sigma_{\text{Distortion}}^2 + \sigma_{\text{TDC}}^2$$

Time resolution is affected by:

- each step in the read-out process
- any effect that changes the shape of the signal

Time resolution

$$\sigma_t^2 = \sigma_{\text{Time walk}}^2 + \sigma_{\text{Landau noise}}^2 + \sigma_{\text{Jitter}}^2 + \sigma_{\text{Distortion}}^2 + \sigma_{\text{TDC}}^2$$



- Variation in time of arrival due to different signal amplitudes
- Can be compensated by electronics

- Caused by inhomogeneous:
 - drift velocity
 - weighting field
- Solutions:
 - saturated drift velocity
 - optimised geometry

TDC: time-to-digital converter

$$\sigma_{\text{TDC}} = \Delta T / \sqrt{12}$$

comparator
time bin width

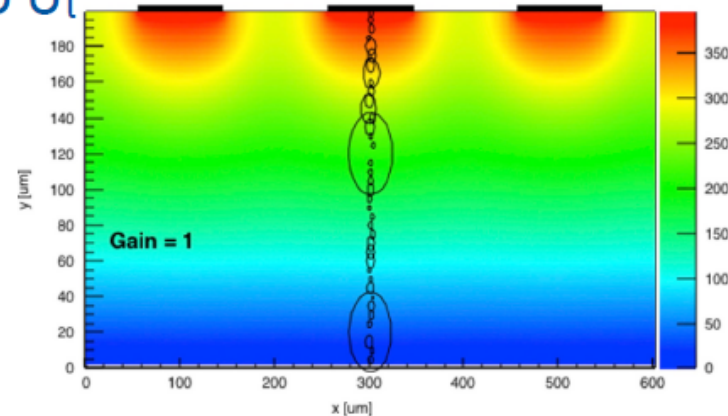
- Sub-picosecond
⇒ negligible

- V_{th} : threshold voltage to determine the time of arrival
- $N\sigma_n$: the threshold is usually expressed in multiples of the system noise

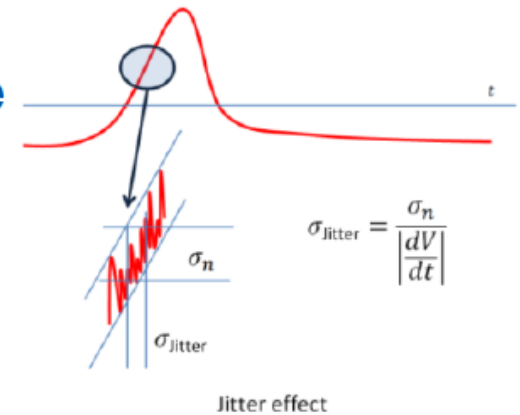
Time resolution

$$\sigma_t^2 = \sigma_{\text{Time walk}}^2 + \sigma_{\text{Landau noise}}^2 + \sigma_{\text{Jitter}}^2 + \sigma_{\text{Distortion}}^2 + \sigma_{\text{TDC}}^2$$

- Signal shape variations for MIPs
 - Non-uniform energy deposition per unit length
- Sets a physical limit to σ_t
- Can be minimised by:
 - setting a low V_{th}
 - using thin devices



- Variations in time of arrival due to signal noise



- Can be minimised with:
 - low noise sensors
 - low noise electronics
 - fast slew rates

- V_{th} : threshold voltage to determine the time of arrival



4-D Ultra-Fast Si Detectors in pCT



In support of Hadron Therapy, the relative stopping power (RSP) is being reconstructed in 3D.

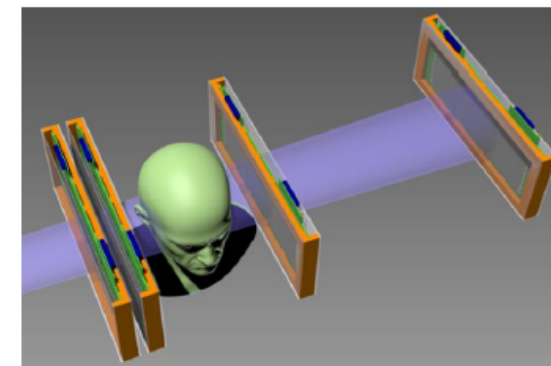
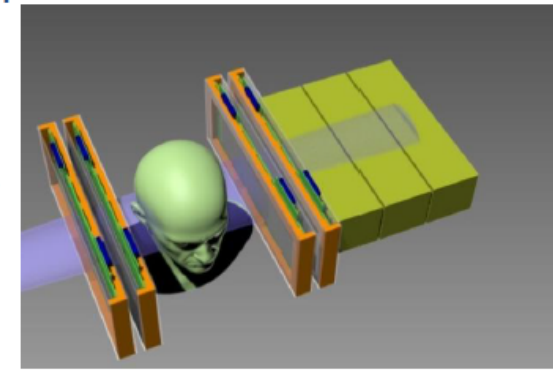
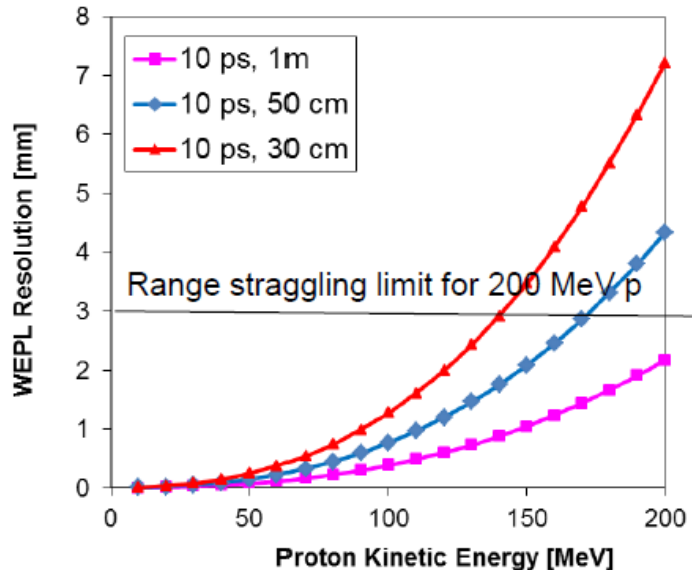
The UCSC-LLU pCT scanner uses Si strip sensors to locate the proton and heavy scintillator stages to measure its energy loss (WEPL).

Protons of 200 MeV have a range of ~ 30 cm in plastic scintillator. The resulting straggling limits the WEPL resolution.



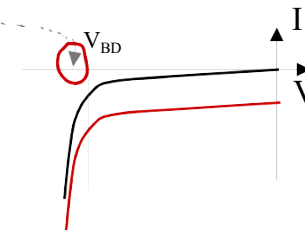
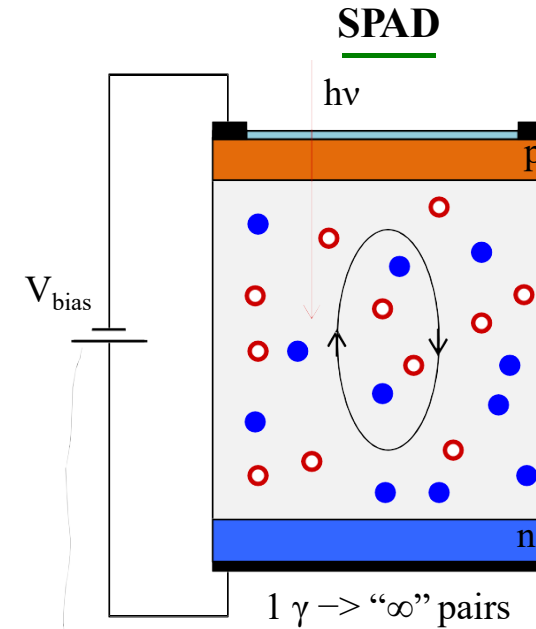
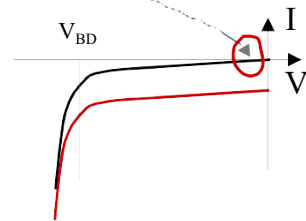
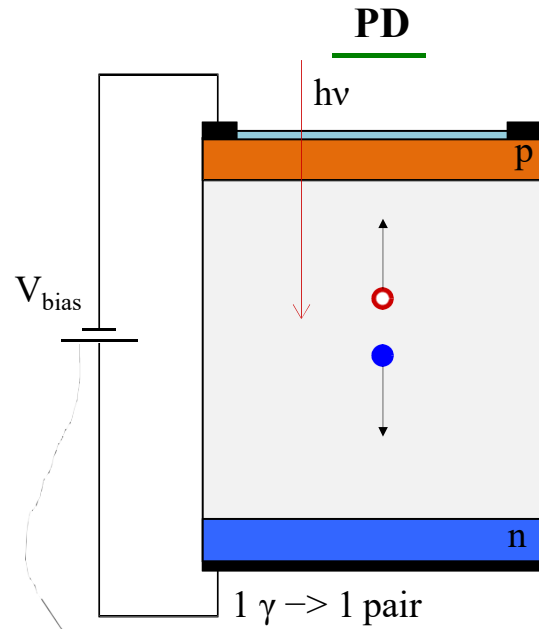
Replace calorimeter/range counter by UFSD:

Combine tracking with WEPL measurement where the ToF of the proton measures the residual energy., with comparable or better resolution than the scintillator.

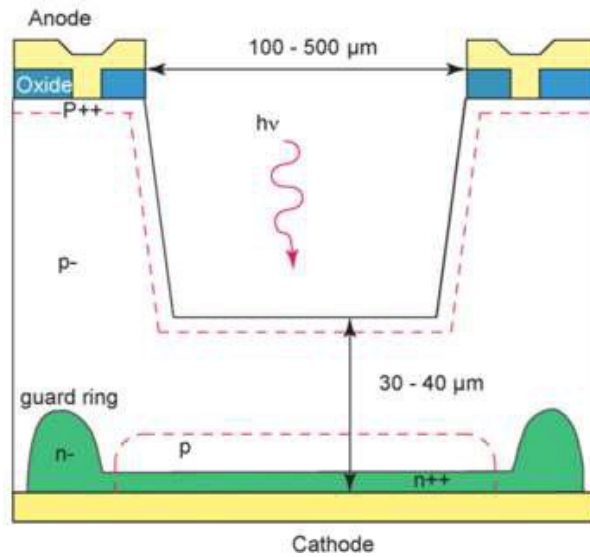


Light-weight,
all silicon
construction
ideal for
installation
Into the gantry

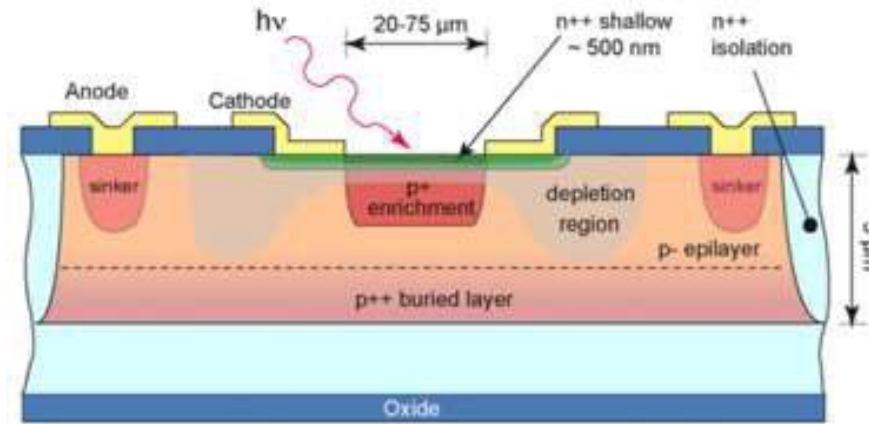
PD and SPAD



Structure of a SPAD



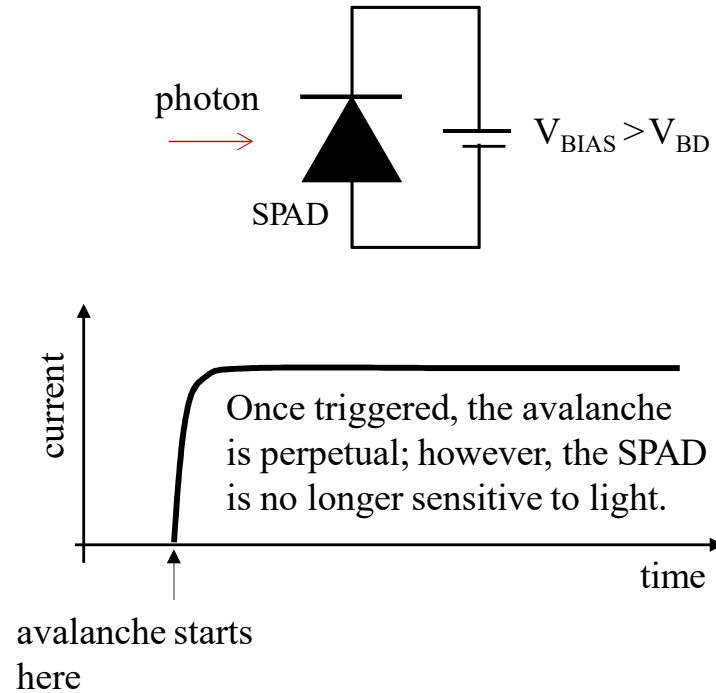
Structure of a *thick* SPAD



Structure of a *thin* SPAD. This structure is used in SPAD arrays.

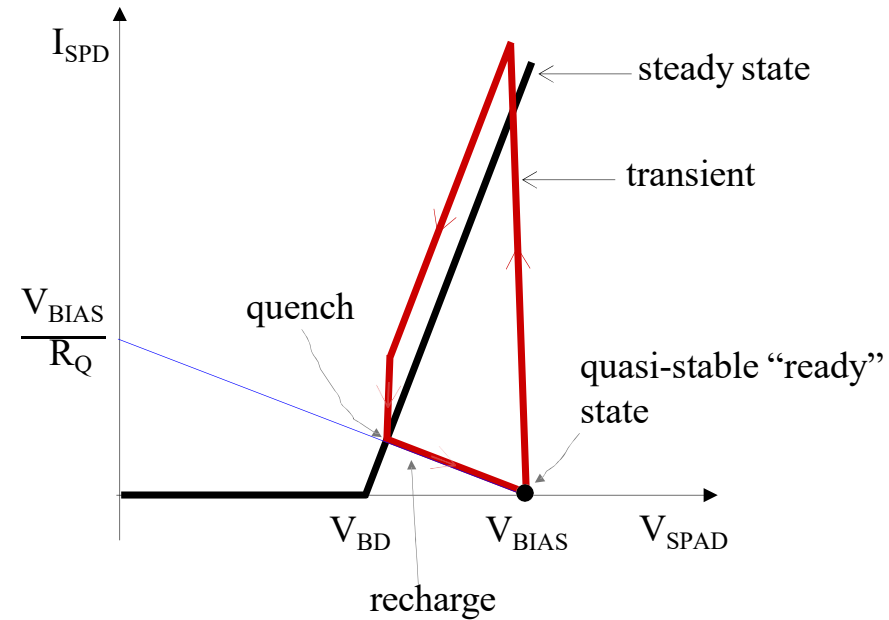
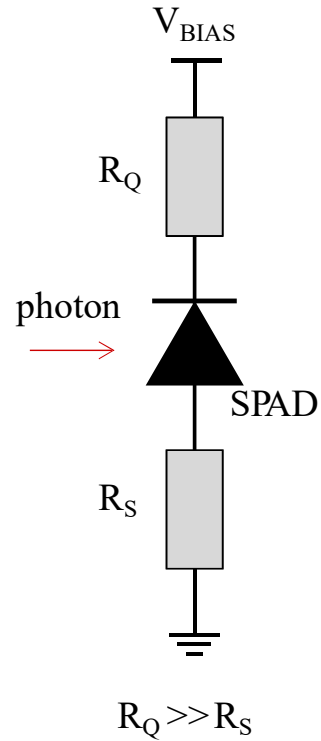
Figures from Zappa et al. 2007

Operation of a SPAD



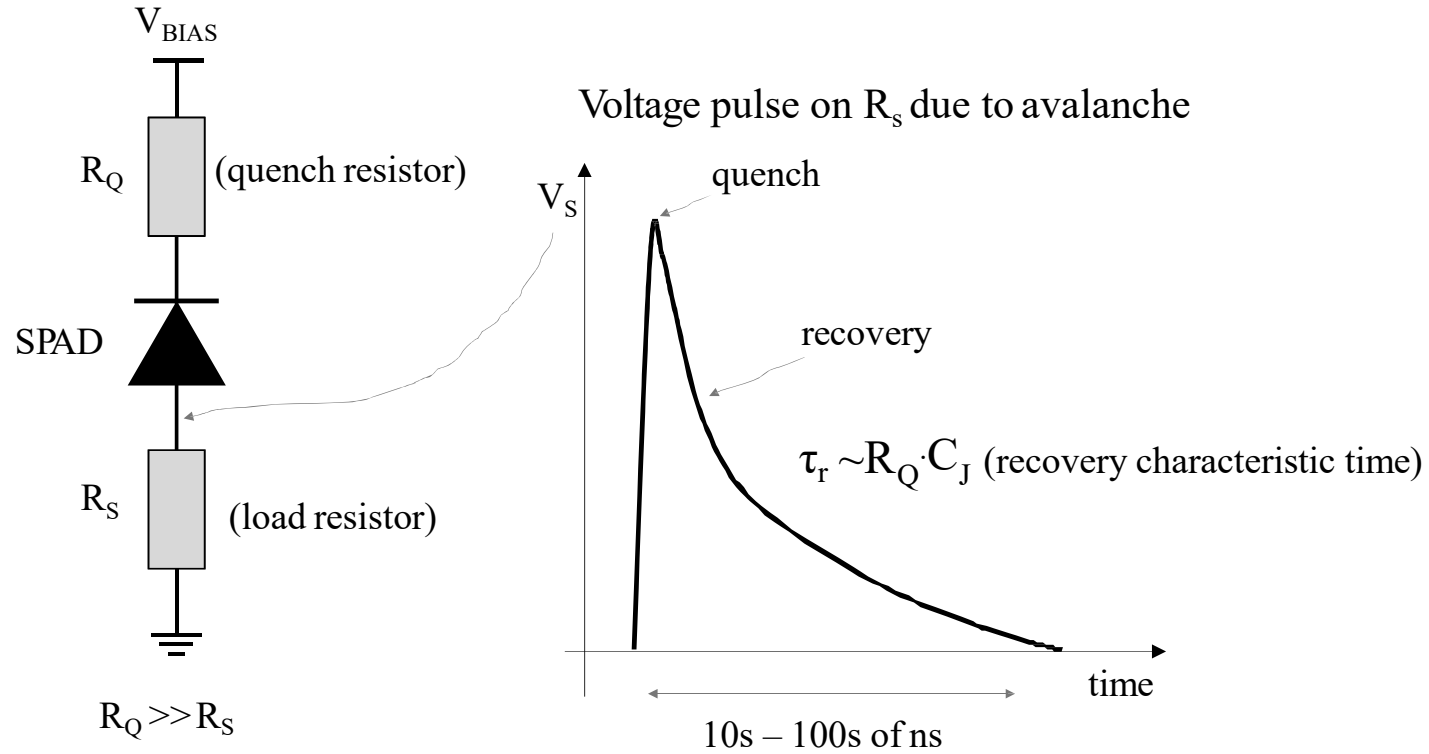
Without quenching, SPAD operates as a light switch.

Operation of a SPAD (passive quenching)

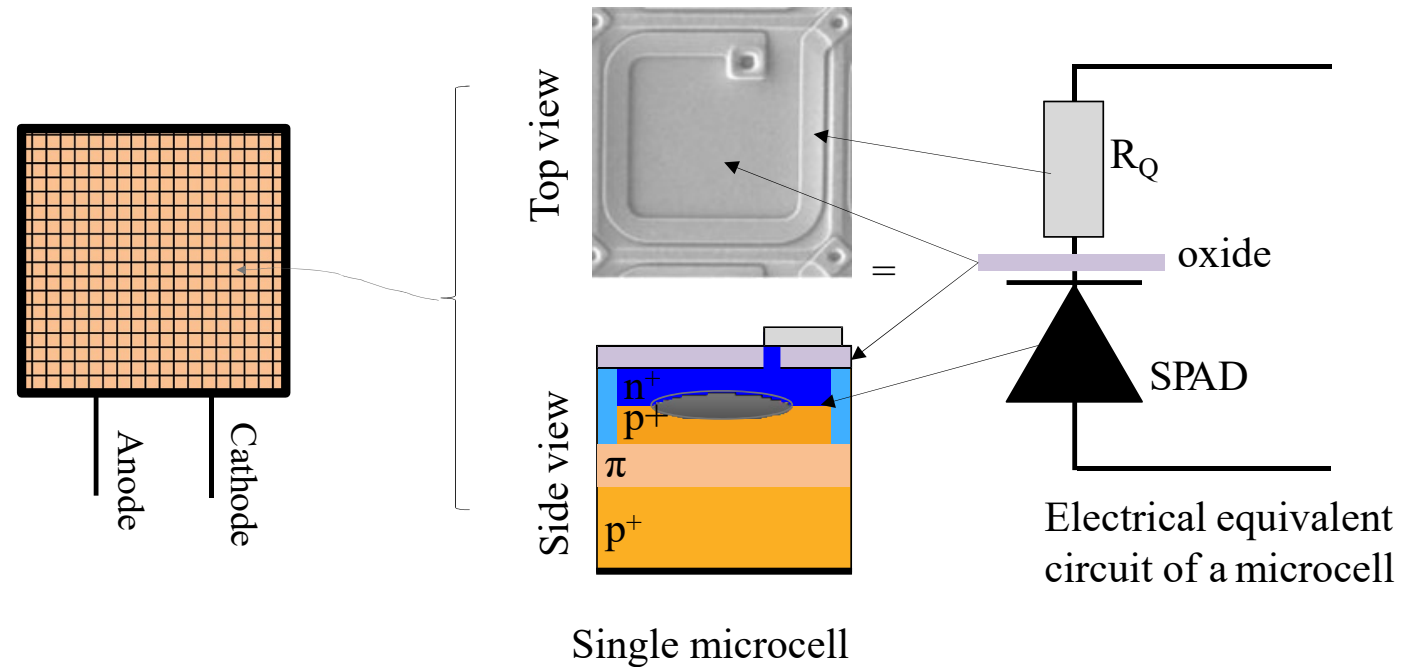


R_Q must be large enough to ensure quenching.

Operation of SPAD (passive quenching)

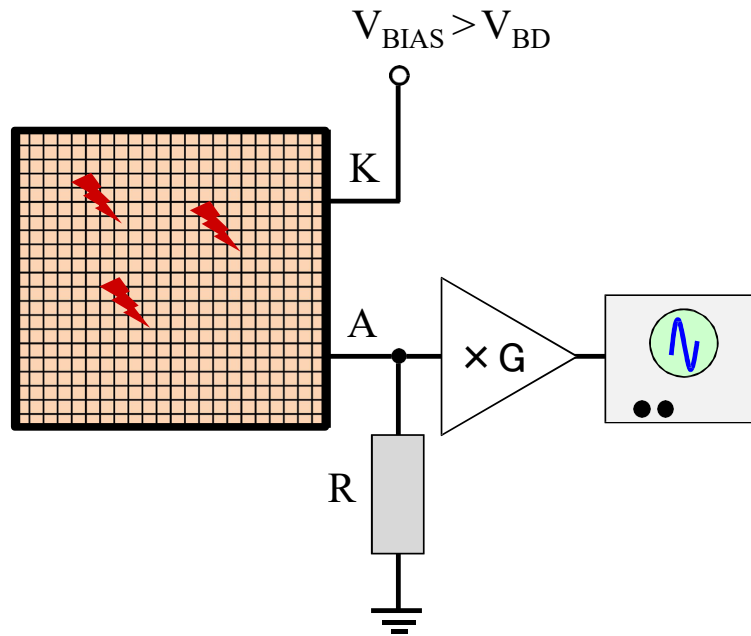


Si-PM Silicon photomultiplier: structure

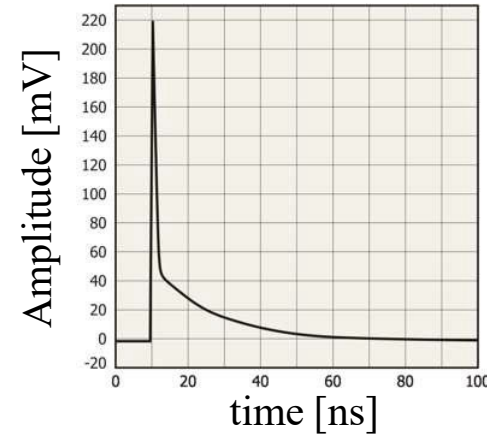


Each microcell is a SPAD in series with a quench resistor. All microcells are connected in parallel. SiPM is **not** an imaging device because all microcells share a common current summing node.

Silicon photomultiplier: operation



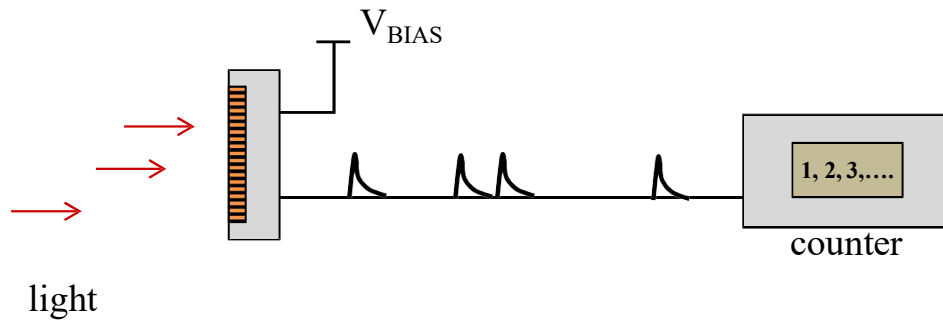
Overvoltage, $\Delta V = V_{BIAS} - V_{BD}$



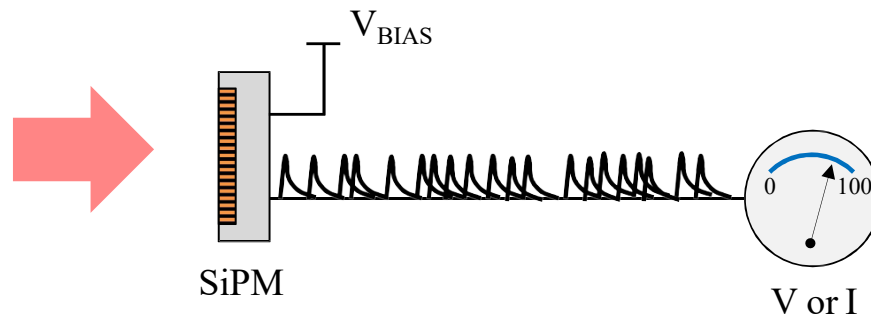
Example of single-photoelectron waveform (1 p.e.)

Gain = area under the curve in electrons

Silicon photomultiplier: modes of operation



If the pulses are distinguishable, SiPM can be operated in a **photon counting** mode.

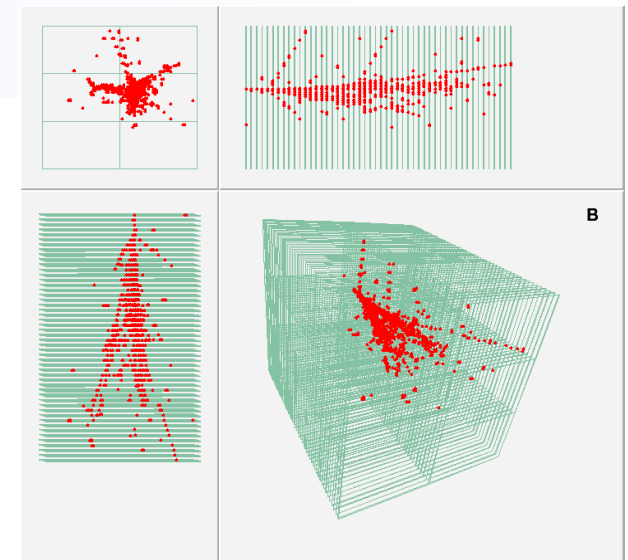
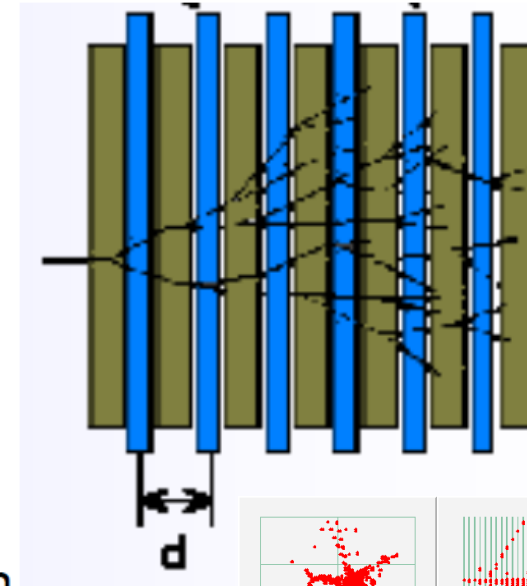


If the pulses overlap, the SiPM can be operated in an **analog mode**. The measured output is voltage or current.

- Applicazione rivelatori al silicio in calorimetria:
 - Calorimetri a campionamento

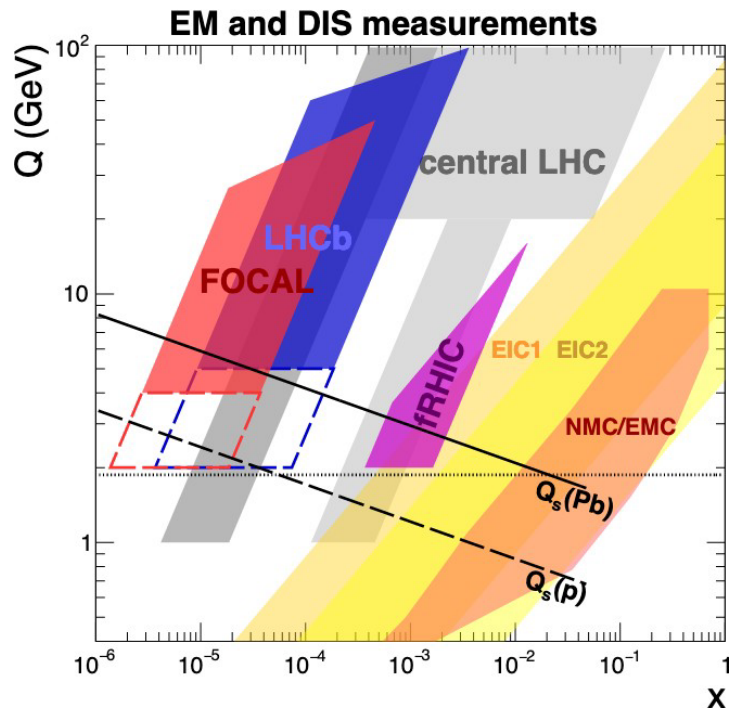
Sampling calorimeters

- Use different media
 - High density absorber
 - Interleaved with active readout devices
 - Most commonly used: sandwich structures →
 - But also: embedded fibres,
- Sampling fraction
 - $f_{\text{sampl}} = E_{\text{visible}} / E_{\text{total deposited}}$
- **Advantages:**
 - Cost, transverse and longitudinal segmentation
- **Disadvantages:**
 - Only part of shower seen, less precise

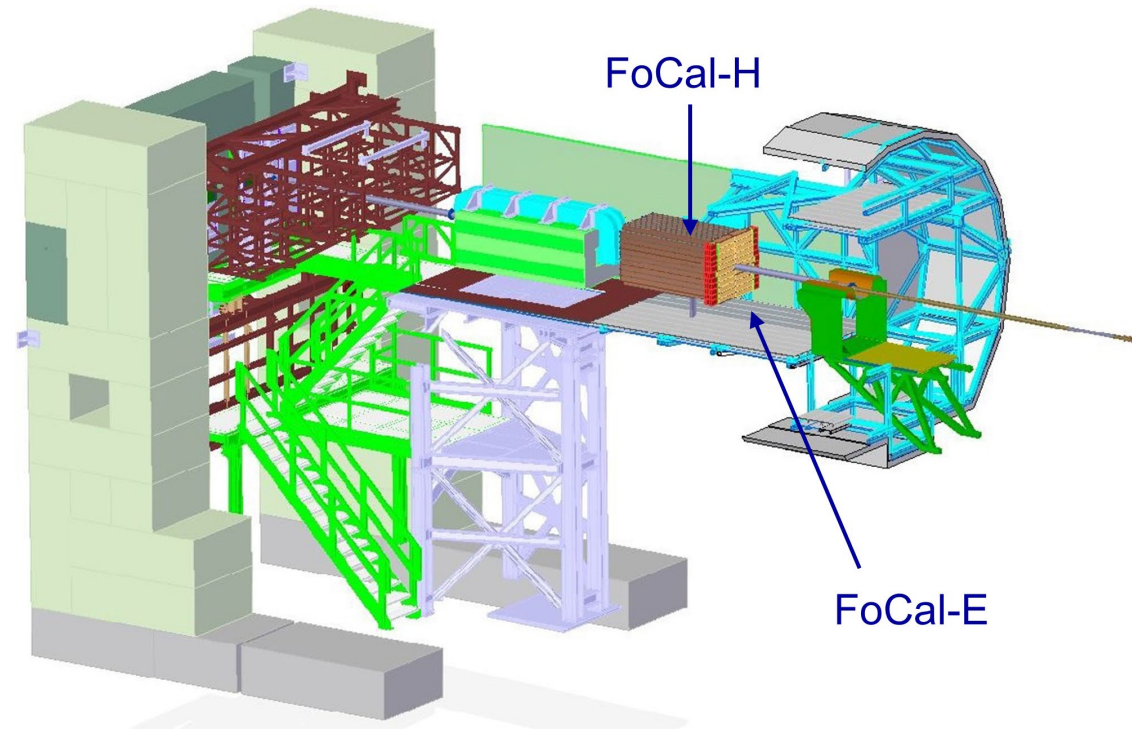


Forward Calorimeter

- Physics Goal: unravel nucleus structure at small-x
 - Unique capabilities to measure **direct photons** in pp and p-Pb
 - Study the **gluon distributions** at **small-x** scale and **low Q**



FoCal LoI - [CERN-LHCC-2020-009](https://cds.cern.ch/record/2710000/files/CERN-LHCC-2020-009)



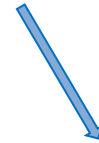
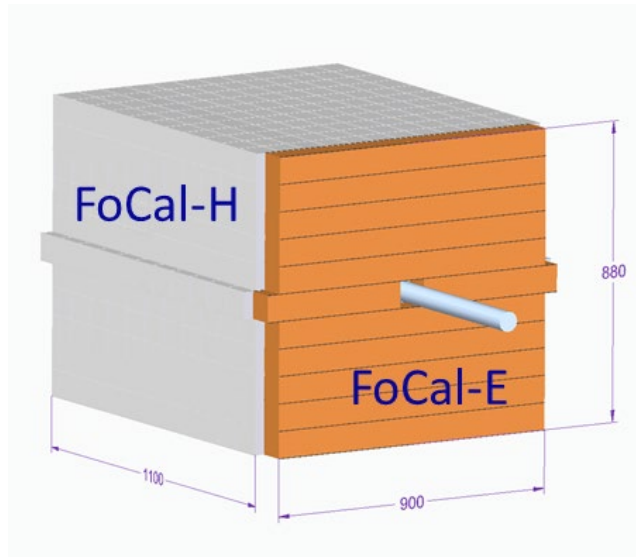
$3.4 < \eta < 5.8$
(baseline design @ 7 m from IP)

FoCal-H and FoCal-E

FoCal-H: Conventional sampling hadronic calorimeter (Cu + scintillating fibres)

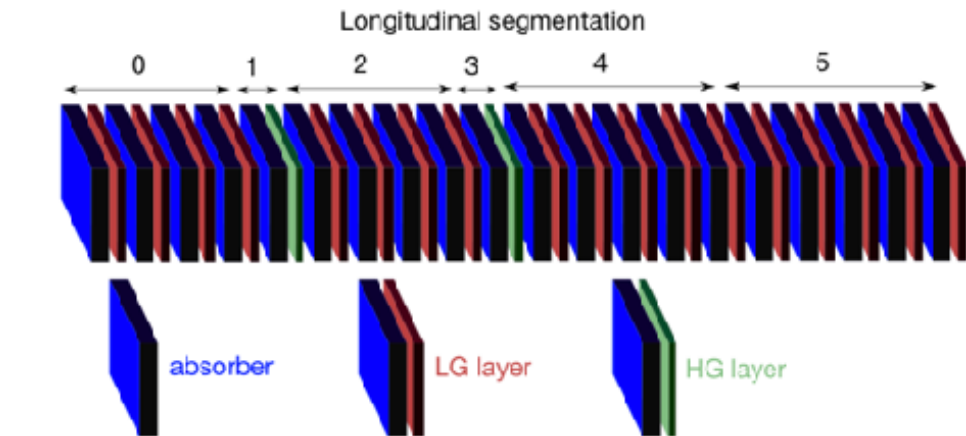
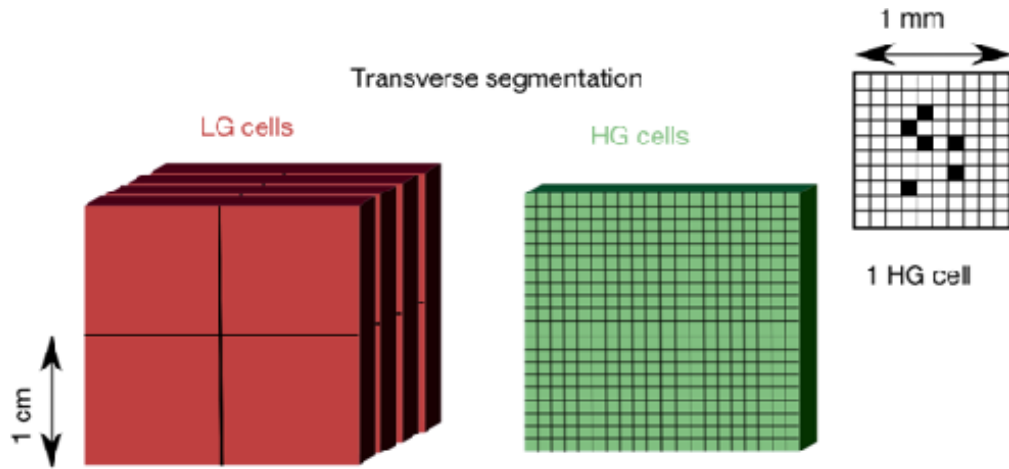
- Providing γ isolation through direct detection of high energy hadrons

FoCal-E: high-granularity Si-W electromagnetic calorimeter for γ and π_0



- **Main challenge** for Focal-E: γ/π_0 separation at high energy
 - two photon separation from π^0 decay: ~ 2 mm
 - needs small Molière radius and high granularity readout
- Si-W calorimeter with effective granularity of ~ 1 mm²

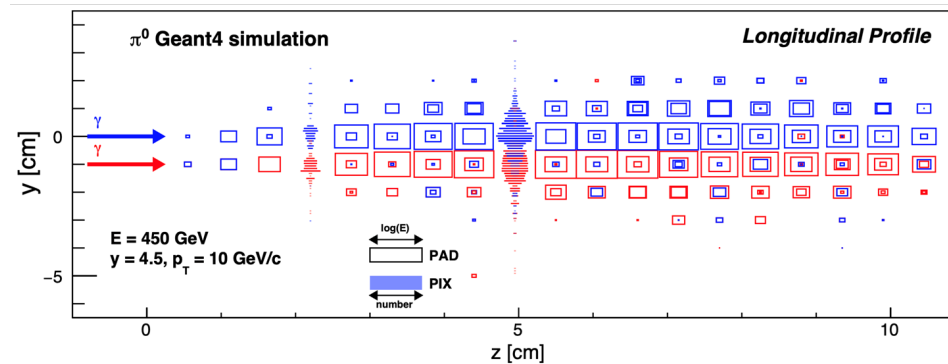
FoCal-E detector technologies



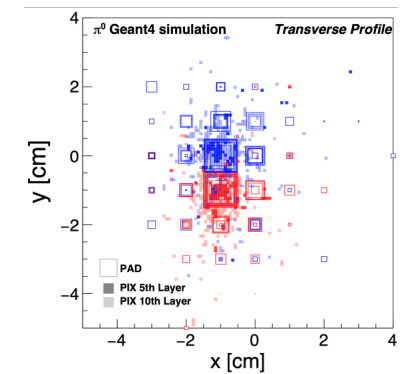
Studied in simulations: 20 layers
W (3.5 mm $\sim 1X_0$) + silicon

- 18 Pad layers
 - Low granularity (LG), provide shower profile and total energy
- 2 Pixel layers (ALPIDE)
 - High granularity (HG), provide position resolution to resolve overlapping showers

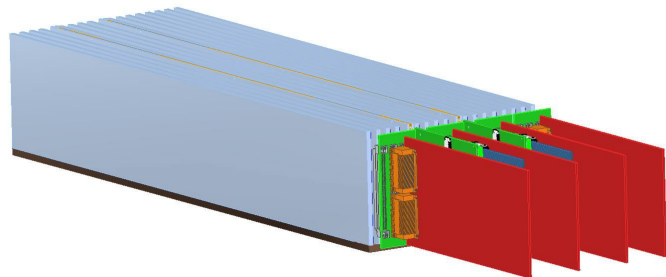
Longitudinal profile (2 γ showers)



Trans. profile

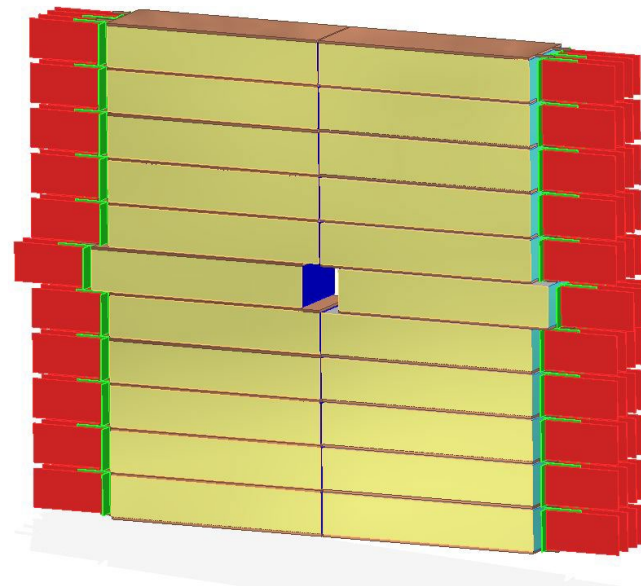


FoCal-E layout and prototypes

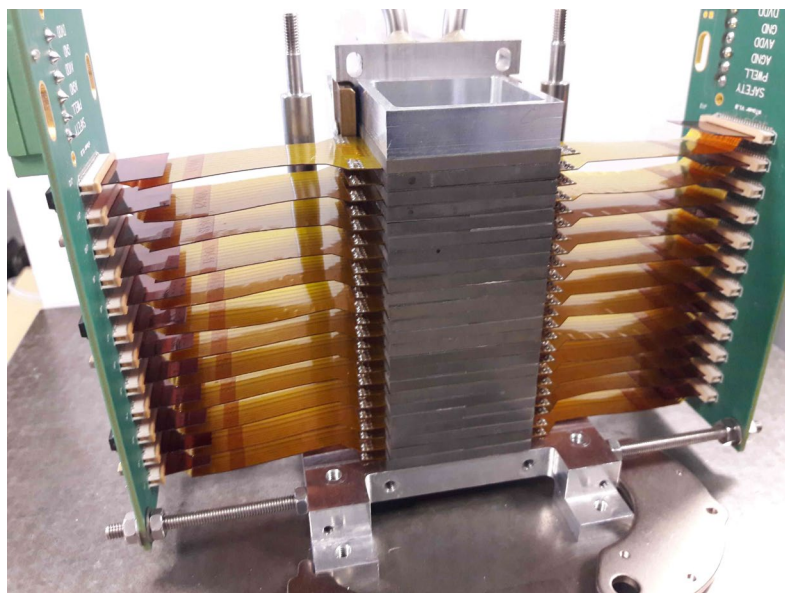


Module: 18 pad layers + 2 pixel layers

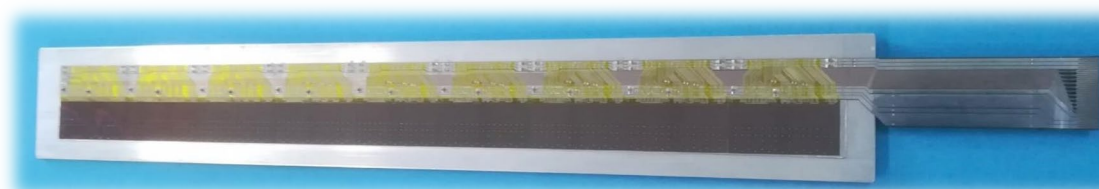
- Readout, power, cooling connected on one side



FoCal-E:
22 modules



EPICAL
all-pixel small E-cal



Pixel string prototype: 9x SpTAB bonded ALPIDE
Final pixel layer will have 3x 15-ALPIDEs strings